

# Plasma impurity co-bombardment effects on sputtering of Beryllium and Tungsten

E. Safi<sup>a</sup>, A. Zitting<sup>a</sup>, K. Nordlund<sup>a,b</sup>

<sup>a</sup>*University of Helsinki, Department of physics, PO Box 43, 00014 University of Helsinki, Finland*

<sup>b</sup>*National Research Nuclear University MEPhI, 31, Kashirskoe sh., 115409, Moscow, Russia*

\* Corresponding author.

E-mail address: [elnaz.safi@helsinki.fi](mailto:elnaz.safi@helsinki.fi) (E. Safi).

## Abstract

In the upcoming fusion device ITER, main plasma-facing materials (PFMs) will be tungsten (W) and beryllium (Be). Fuel and impurity plasma ions as well as lead to sputtering of PFMs. The typical impurities include Be eroded in the main chamber as well as nitrogen (N), argon (Ar) and neon (Ne) often used for power exhaust schemes based on detachment [<https://doi.org/10.1016/j.nme.2017.03.033>]. To study the effect of plasma impurities on the erosion and surface morphology of wall materials, molecular dynamics simulations were carried out. Therefore, we modelled irradiation of both W and Be surfaces with Ar-deuterium (D) and Ne-D mixtures, varying the fraction of Ar and Ne impurities from 0 to 20 percent with impact energies of 10-100 eV at 500 and 800 K surface temperatures for W and impact energies of 30-200 eV at 400, 600 and 800 K surface temperatures for Be. In both materials, after a few hundred bombardments, the sample surface was damaged and cell structures changed from crystalline to amorphous at lower ion energy and a blistering-like effect was observed due to D<sub>2</sub> accumulation in the Be cells at higher energies. Due to the sputtering threshold in W only the heavier noble gas impurities were responsible for surface erosion in the energy range studied here, and the dominating sputtering mechanism was physical region. For Be at impact energies higher than 100 eV, total Be sputtering yield, in the presence of Ar or Ne impurities, is around three times higher than pure deuterium irradiations. The effect of surface temperature on the results was shown to be negligible.

## 1. Introduction

, ITER [1] will be the world's largest and the most advanced tokamak fusion device aimed to demonstrate a net excess of fusion energy, in deuterium (D)- tritium (T) plasmas [2]. Extreme conditions such as

particle flux, thermal loads and temperature at locations determined by ITER design may lead to critical material damage and thus, plasma-facing component lifetime issues affecting the availability of ITER and its duty cycle. Moreover, erosion affects retention of tritium due to co-deposition (mainly with Be). T retention in ITER should not exceed safety limit of 1kg. Therefore, selecting appropriate materials for different plasma facing components (PFCs) of the device is critical. Therefore, simulation of reliable data for relevant erosion processes is of importance.

ITER will have a full metallic wall comprised by tungsten (W) plasma-facing components (PFCs) in the divertor area and beryllium (Be) PFCs in the main wall. On the one hand, W is selected because of its high sputtering threshold and low fuel retention [3]. Moreover, W has advantages power-handling due to its high melting point. On the other hand, Be has been chosen as low-Z element helpful to minimize the core plasma radiation (dangerous for both energy confinement and plasma stability), fuel retention (in comparison to carbon) [<https://doi.org/10.1016/j.jnucmat.2014.12.007>] and its oxygen gettering properties [2,4].

As a result of non-perfect plasma confinement by magnetic field, PFCs will be exposed to D ions from the plasma which cause sputtering of wall materials.. Moreover, to reduce the particle and local power load onto wall materials, impurity seeding is often used as a method to reduce an excessive heat flux [6] [<https://doi.org/10.1016/j.nme.2017.03.033>] [7] by deliberate seeding of gas impurities (N<sub>2</sub>, Ar, Ne, etc) into the divertor. This can be achieved manually by puffing noble gas impurities in the ITER vacuum vessel.

[8-10]. [8]. Therefore, investigating the interaction of plasma impurities such as H/D/T, Be, Ne and Ar with W and Be PFCs and understanding the underlying mechanism is vital. The influence of these impurities on the PFM erosion, including the effects due to surface morphology evolution during the plasma irradiation is the focus of the present work.

Previously, the effect of plasma impurities on the sputtering of tungsten carbide (WC) was studied by molecular dynamics (MD) simulations [11]. For that purpose, cumulative irradiation of D with C, W, Ne, He and Ar impurities on WC surfaces was studied. The results showed a higher sputtering yield for W and C in the presence of impurities rather than pure D irradiation. In addition, preferential C sputtering was observed during the irradiations.

Sputtering of pure Be, W and Be-W mixed materials exposed to D ion has been studied extensively both by experiments (in tokamaks as well as linear plasma devices) and modeling [5, 12-18]. Moreover, the effect of Ar as a plasma impurity on erosion and fuel retention for Be in the PICES-B linear plasma device [6] and the influence of mixed D + Ne or D + Ar impurities on D permeation in W in high flux ion beam test device (HiFIT) [10] were studied experimentally. However, a complete description of the effect of Ar and Ne impurity in D plasma on the sputtering and surface morphology changes of pure W and Be surfaces had not been achieved yet.

The aim of the present work is to improve the understanding of the effect of plasma impurities on W and Be surface erosion and morphology by MD techniques and calculate corresponding yields. In this work, we used different fractions of plasma impurities Ar and Ne in addition to D ions, and therefore performed mixed-ion impacts on W and Be, scanning over fusion relevant parameters such as impact energies and substrate temperatures. Special attention is given to the magnitude of W and Be sputtering yields caused by different fractions of plasma impurities.

## 2. Method

MD is a computational method capable of describing bond formation and breaking when appropriate reactive interatomic potentials are used. Therefore, it is a great technique to study the erosion of chemically active structures. The code PARCAS [19] was used for all MD simulations presented in this work, using the Juslin et al. potential [20] for the W system and the related Björkas et al. potential for Be system [21]. The interaction models used between noble gas (Ar and Ne) and W, Be and D atoms were pair potentials of the Ziegler-Biersack-Littmark (ZBL) type [22].

The simulations were performed in two main steps: first the initial structures of pure W and Be were created, and then the cells were irradiated with 2000 mixed Ar+D and Ne+D ions at normal incidence cumulatively.

The initial structures for W and Be simulations were created by relaxing a body-centered cubic (BCC) structure for W and, a hexagonal closed packed (HCP) structure for Be at desired substrate temperatures, also opening a perfectly flat (001) and (0001) surface normal to the z-direction for W and Be, respectively. 2000 cumulative impurity bombardments with a mixture of  $x\%$  Ar or Ne with  $(100-x)\%$  D

( $x=0, 5, 10$  &  $20$ ) were performed on both W and Be surfaces, varying the impact energy and substrate temperature. During the irradiation events the impinging ion species was randomly chosen. The characteristics of each simulation cell and mixed ion impact parameters are listed in Table 1.

The starting point of the impact ion was set to be 5 Å above the surface and the impact point was varied in each irradiation, by randomly shifting the cell in the  $X$  and  $Y$  directions. The temperature and pressure was controlled by using Berendsen's method [23] at the borders and bottom of the cell during the simulations. Periodic boundary conditions were applied in the  $X$  and  $Y$  directions and the bottom layers were fixed.

Further details regarding the methodology, use of PBCs, electronic stopping and treatment of sputtered and backscattered particles, can be found in ref. [24]

## **3. Results**

### **3.1 Tungsten**

Tungsten total erosion yields obtained from our D co-bombardment with Ar and Ne ions as a function of impact energy at two different surface temperatures are shown in figure 1. W sputtering yields for pure D bombardments were zero for the cases studied here due to the high D sputtering threshold. Therefore, Ar and Ne impurities are the only ones responsible for W erosion in the divertor region at lower impact energy. For impact energies higher than 50 eV, W sputtering increases with both energy and impurity concentration. There seemed to be no statistically significant temperature dependence on W sputtering. Moreover, the W molecular sputtering yield is really low, which is not enough for statistical analysis here.

The fraction of D atoms that were not implanted in the W cell, but instead reflected back from the surface for different surface temperatures are plotted in figure 2, as a function of impact energy for both pure D and Ar and Ne mixed bombardments with D. Those atoms were either reflected from the surface or released as molecules. Deuterium reflection clearly decreases with increasing ion energy. This is simply due to increased kinetic energy making it easier to penetrate into the material instead of reflecting from the surface. The effect of temperature seems minimal at higher energies, but there is a clear difference at lower energies. Additionally, higher impurity concentration seems to increase the deuterium reflection at higher energies with very little impact at the lower ones. This could be due to the increased surface

damage caused by impurities at higher energies leading to more D reflection.

Reflection of noble gas impurities was 100% for all Ar cases while some Ne cases had reflection of slightly less than 100% but no more than 97% (Fig. 3). Ar ions seemed to be unable to penetrate into the surface, while some Ne ions penetrated just deep enough where they could act as substitutional defects in the tungsten lattice. However these Ne impurities were not stable in W interstitial sites and prefer to move to other nearby vacancies if possible. Once near the surface they would escape the lattice completely.

### 3.2 Beryllium

During ion bombardment on the Be surface, both single Be atoms and Be molecules (mostly BeD) were eroded from the sample. The total Be erosion yield as a function of impact energy for a different amount of Ar and Ne at different surface temperatures are given in figure 4. In both Ar and Ne cases at 600K and 800K surface temperature, the yields for 100% D impacts are added to all the graphs presented in this section for a better comparison. The results clearly show how impurity co-bombardments of Be cells at different surface temperatures and impact energies affect the Be erosion behavior. With increasing the fraction of noble gases, sputtering yields were increased within the error bar for impact energies higher than 100 eV. Moreover, a different surface temperature doesn't have a significant effect on Be sputtering when noble gas impurities are added to D bombardments in comparison with pure D ion bombardments [17].

Figure 5 shows sputtering yield of BeD<sub>n</sub> molecules as a function of impact energy at different surface temperatures for both Ar and Ne mixed bombardments with a D plasma. The effect of noble gas impurities on BeD<sub>n</sub> molecular sputtering is less significant here. The sputtering yields for different amount of Ar and Ne during simulations, follow almost the same trend as in pure D simulations. The yields increased with impact energy with a peak at 100 eV, but reduced for energies larger than 100 eV (in the range studied here) because of higher D penetration depth. It should be noted that among the sputtered species there were around 10% BeD<sub>2</sub> molecules of all BeD<sub>n</sub> molecules in both Ar and Ne mixed bombardment, and the rest of the molecular species were BeD molecules.

Figure 6 illustrates total D reflection yield from the Be surface as a function of impact energies for pure D and mixed impurity bombardments at temperature ranges studied here. Those atoms were either reflected from the surface or released as molecules. With increasing impact energy, the fraction of

reflected D atoms reduced. For energies higher than 100 eV, a large fraction of D atoms went through the simulation cell and were retained in the bulk. At lower impact energies, a higher amount of D atoms were reflected from the surface, which there is a smaller amount of Ar and Ne impurities. It should be noted that release of molecular D was found to be minor. Moreover, the effect of surface temperature on D reflection was found to be negligible.

The noble gas atoms were mostly reflected back from Be surface rather than accumulating in the sample (Fig. 7). At highest impact energy, 200 eV a few percent of Ar and Ne were implanted in Be cell due to higher ion penetration depth.

## **4. Discussion**

### **4.1 Impurity effect on sputtering**

W sputtering yields for pure D irradiations are zero for the energy range studied here. These findings described that adding a few percentage of impurities to D ions can significantly affect W total sputtering yields, specially at higher energy of the impurity ions, which correlates well with previous experimental and modeling works [8, 11]. Moreover, impurity bombardment on Be surface results in higher Be sputtering yields, and increasing the energy of impurity ion increased single Be sputtering yields. At impact energies lower than 50 eV, adding noble gas impurities to D bombardments would not significantly affect W and Be erosion yields. Furthermore, the sputtering mechanism in low ion irradiation energy range is due to swift chemical sputtering phenomena [15], and large atoms such as Ar and Ne have a very low probabilities to cause swift chemical sputtering. However, noble gases affect the total erosion of both W and Be targets significantly at impact energies higher than 100 eV where physical sputtering is possible. These findings correlate well with another MD modelling of H, He, Ne, Ar-bombardment of amorphous hydrocarbon structures, performed by Träskelin et. al. [25].

There were a few cases of WD molecular sputtering which is not enough for statistical analysis, however the existence of multiple such events is still an important result. In the mechanism of WD sputtering, a single D atom was bound to nearby W atoms and the next incoming impurity ion have enough energy to break W-W bonds and knocks the W atom away from the surface with D atom that was bound to it, causing a WD molecule to be sputtered. This combined with the high energies of the impurities means that the WD sputtering mechanism is likely physical rather than chemical.

## 4.2 Materials modification

During ion irradiations, the structure of both W and Be samples were changed. At energies of 50 eV and below, amorphization of the W and Be samples were observed as the irradiation went on, the deuterium ions gathered at the surface, changing the structure from crystalline to non-crystalline due to the high concentration of deuterium.

For W simulations, at higher energies the surface itself remained almost completely intact during pure D bombardment, with damage forming deeper in the lattice. However, when noble gas impurities were introduced, at higher impact energies the surface experienced notable damage, it remained crystalline, but became much rougher. The amount of damage the surface received increased with both ion energy and impurity concentration.

Figure 8 represents W surface structures at 800K surface temperature due to 10% Ne-90% D co-bombardments at different impact energy. The structures show that the D penetrates deeper into the surface with increasing impact energy, and is spread over a wider area. There is also more deuterium, which is consistent with D reflection decreasing with ion energy. Furthermore, the concentration of noble gas impurities seems to have minimal effect on the D depth profile except at higher energies where increased impurity concentration seems to cause slight depletion of D at the surface. The higher impurity concentrations lead to an increasing D reflection yield, therefore the damage caused to the surface prevents deuterium atoms build up near the surface.

Figure 9 shows the morphology changes in the Be surface at 600K surface temperature due to 20% Ar-80% D co-bombardments at different impact energy. In this samples, the first few surface layers have become amorphous at lower impact energies (30-50 eV) due to higher D density at the surface, which leads to more bond breaking and formation of Be and D at temperature ranges studied here. For energies lower than 100 eV, a large fraction of D atoms and almost all the irradiated noble gases, were reflected back from surfaces. For ion impact energies higher than 100eV, and therefore higher ion penetration depth, a large fraction of D atoms went through samples, and a smaller number of Ar and Ne atoms were also implanted, which results in observing amorphization deeper in the simulation cells. For this energy range, the D clustered in the center of the cell, mainly forming D<sub>2</sub> molecules. In a few cases, this D<sub>2</sub> accumulation resulted in the separation of a D<sub>2</sub> layer, where the top layer of the cell was ruptured due to the high D<sub>2</sub> gas

pressure, which can apply a force in z direction. The above layers flew off and the simulation was stopped in this case. Moreover, the blistering mechanism and rupture due to the existence of sufficient amount of  $D_2$  molecules in sample were also reported by Vörtler et al. [11], however, surface rupture in W simulations was not observed here.

It should be noted that, depending on the ion energy, Ar and Ne were also spreading out within both W and Be cells. However, this fraction was low and noble gas atoms did not accumulate in the cell or bind with other atoms to form clusters in simulations.

## **5. Conclusions**

Using MD simulations, we have studied the effect of Ar and Ne impurities irradiation mixed with D on the sputtering and surface morphology changes of pure W and Be surfaces due to D plasma irradiation, as a function of substrate temperature (400-800 K) and impact energy (10-200 eV). Special attention was paid to the magnitude of W and Be erosion yields due to varying content of Ar and Ne plasma impurities. In general, W and Be sputtering yields were higher in the presence of Ar and Ne plasma impurities in compare with pure D ion irradiations and sputtering yield's magnitude increased with increasing impact energy, while the effect of substrate temperatures for the surfaces studied here was negligible. However, noble gases affect significantly the total erosion of both W and Be targets at impact energies higher than 100 eV where physical sputtering is possible. Due to high energy threshold for the deuterium sputtering in heavy high-Z elements, sputtering of W by impurities was significant for the impact energy range studied in this paper.

We found that W and Be surfaces were more damaged at higher impurity concentration. Moreover, D reflection was clearly decreasing with increasing ion energy due to higher kinetic energy and therefore deeper penetration of ions into the surface. A large amount of D ions was implanted in the W and Be cells with increasing ion energy, which results in observing amorphization deeper in the simulation cell. A blistering-like effect and surface rupture was observed in Be. A very small amount of Ar and Ne impurities were implanted in the W and Be cells, i.e. these ions were mostly reflected back from the sample surfaces.

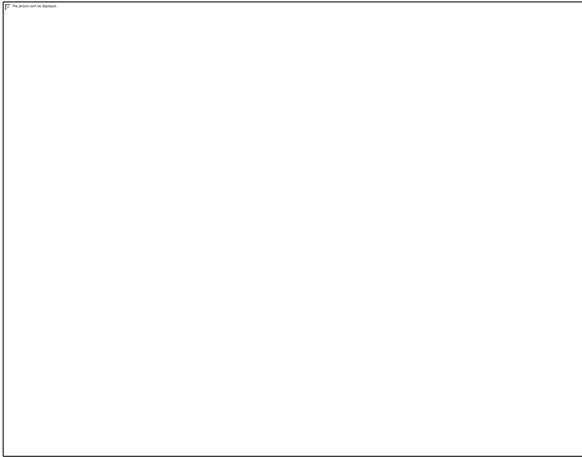
## Acknowledgments

This work has been carried out within the framework of the EUROfusion consortium and has received funding from the Euratom research and training program 2014–2018 under grant agreement No. 633053. The views and opinions expressed herein do not necessarily reflect those of the European commission. Grants for computer time from CSC, the Finnish IT Center for Science as well as the Finnish Grid and Cloud Infrastructure (persistent identifier urn:nbn:fi:research-infras-2016072533), are gratefully acknowledged.

	W	Be
Structure	BCC	HCP
N	3800	2640
Size(nm)	3.2*3.2*6.0	2.3*2.3*4.0
T(K)	500, 800	400, 600, 800
E(eV)	10, 30 , 50, 80, 100	30. 50, 100, 150, 200
Flux ( $10^{28}\text{m}^{-2}\text{s}^{-1}$ )	2.02	2.02

Table 1. Parameter sets used in the 2000 cumulative MD simulations on W and Be surfaces.  $N$  is the number of atoms in the simulation cell,  $size$  refers to the cell dimensions,  $T$  is the substrate temperature,  $E$  and flux are mixed ions impact energy and flux.

(a)



(b)

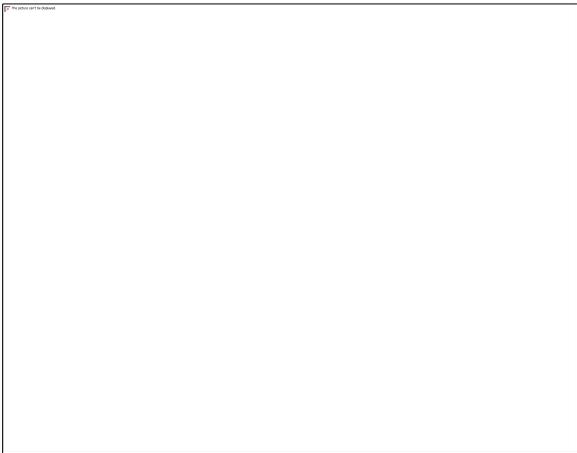


Figure 1. Total W sputtering yield as a function of impact energy at different surface temperature for (a) Ar-D and (b) Ne-D co-bombardments of W cells.

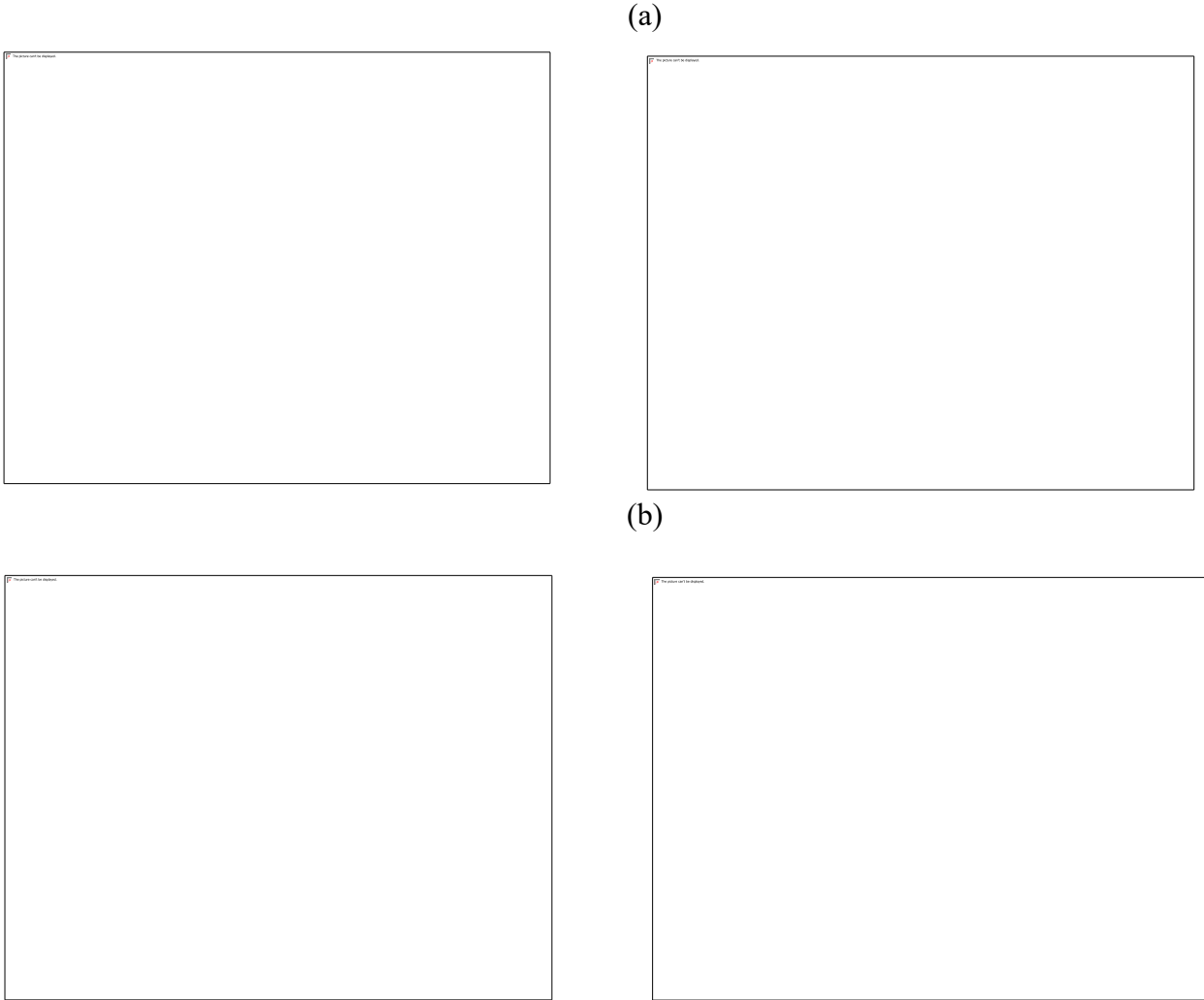


Figure 2. The amount of D atoms that are reflected back (not implanted) from the W cell as a function of impact energy at different surface temperature for (a) Ar-D and (b) Ne-D co-bombardments of W cells.

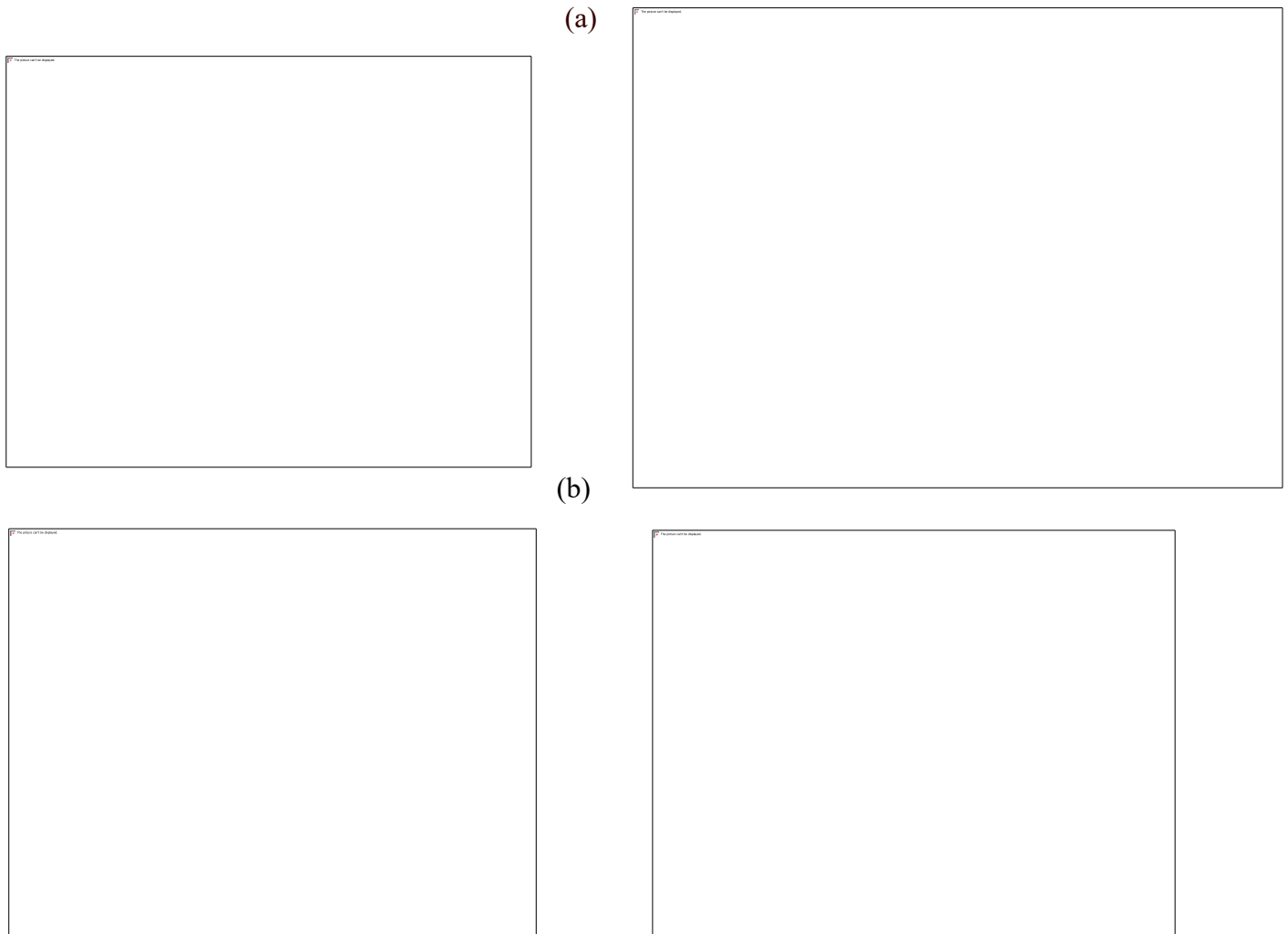


Figure 3. The amount of noble gas atoms that are reflected back (not implanted) from the W cell as a function of impact energy at different surface temperature for (a) Ar-D and (b) Ne-D co-bombardments of W cells. Error bars represent the standard error and are merely an indicator of accuracy rather than range of probable values (since yields of more than 1.0 are impossible in this scenario)

(a)

The number of the person	The number of the person	The number of the person
--------------------------	--------------------------	--------------------------

(b)

The number of the person	The number of the person	The number of the person
--------------------------	--------------------------	--------------------------

Figure 4. Total Be sputtering yield as a function of impact energy at different surface temperature for (a) Ar-D and (b) Ne-D co-bombardments of Be cells.

(a)

(b)

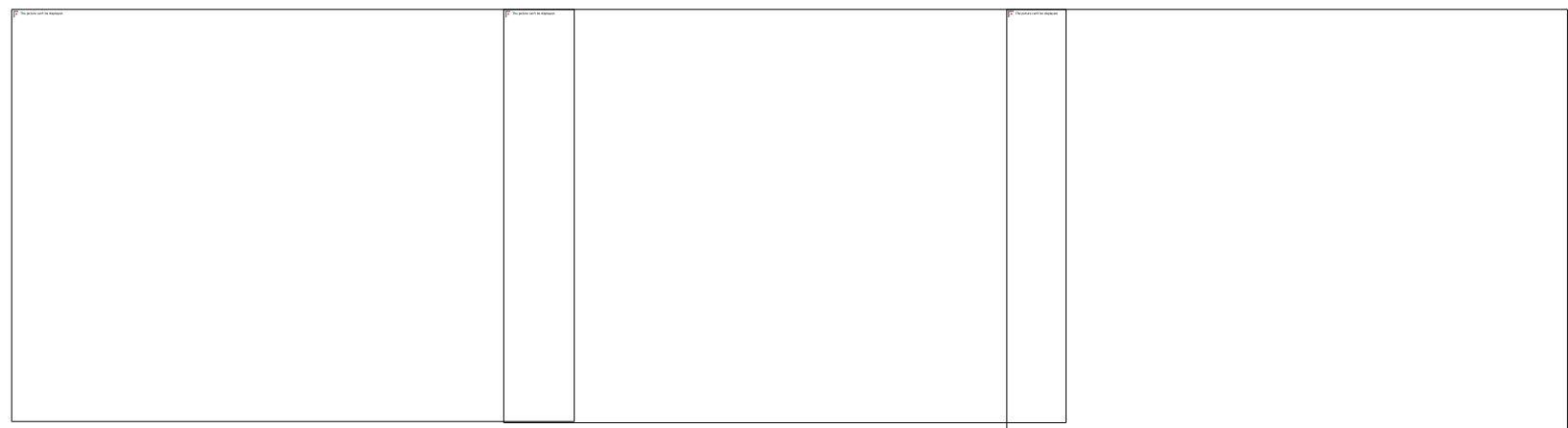
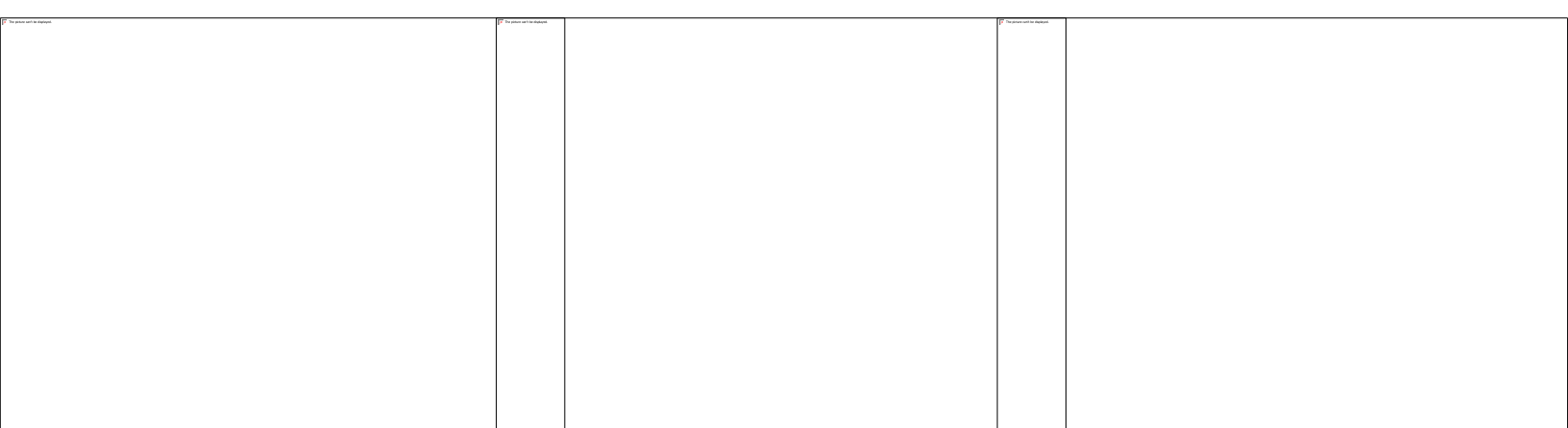




Figure 5. Sputtering yield of  $\text{BeD}_n$  molecules as a function of impact energy at different surface temperature for (a) Ar-D and (b) Ne-D co-bombardments of Be cell.

(a)



(b)

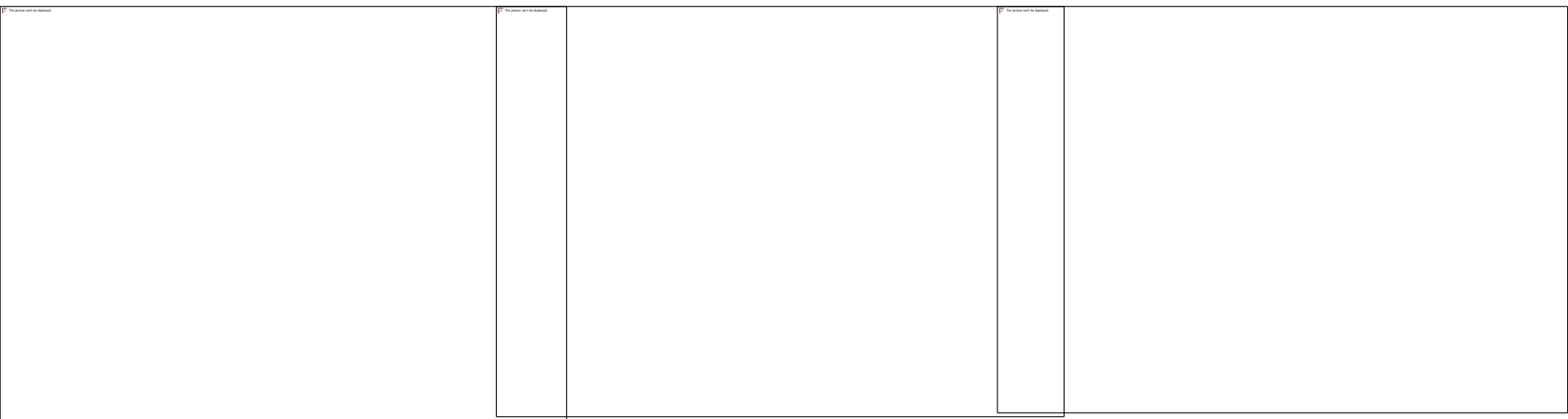


Figure 6. The amount of D atoms that are reflected back (not implanted) from the Be cell as a function of impact energy at different surface temperature for (a) Ar-D and (b) Ne-D co-bombardments of Be cells.

(a)



(b)

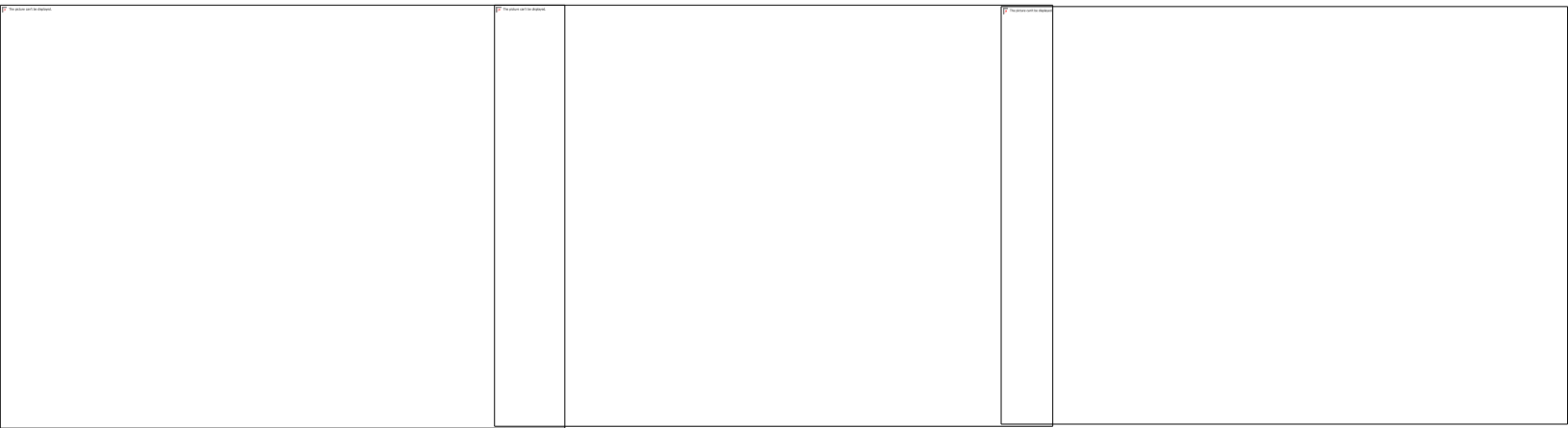
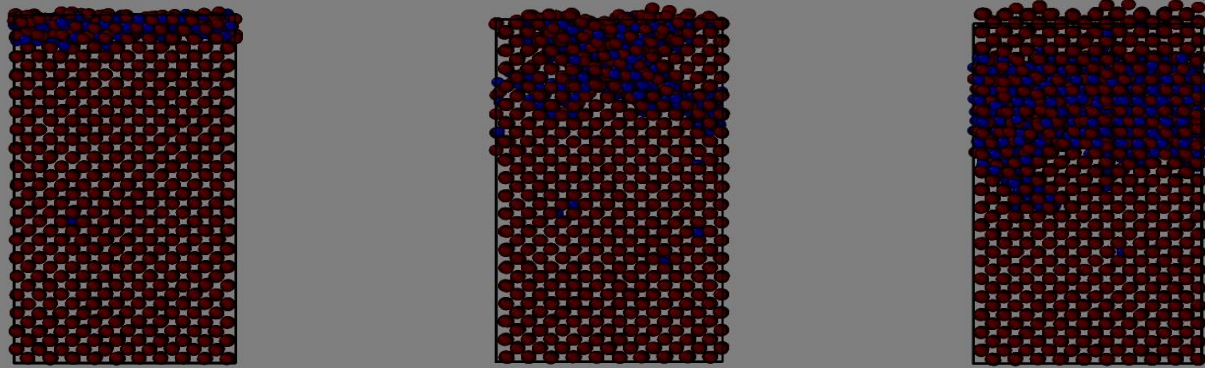


Figure 7. The amount of noble gas atoms that are reflected back (not implanted) from the Be cell as a function of impact energy at different surface temperature for (a) Ar-D and (b) Ne-D co-bombardments of Be cells. Error bars represent the standard error and are merely an indicator of accuracy rather than range of probable values (since yields of more than 1.0 are impossible in this scenario)

10 eV

30 eV

50 eV



80 eV

100 eV

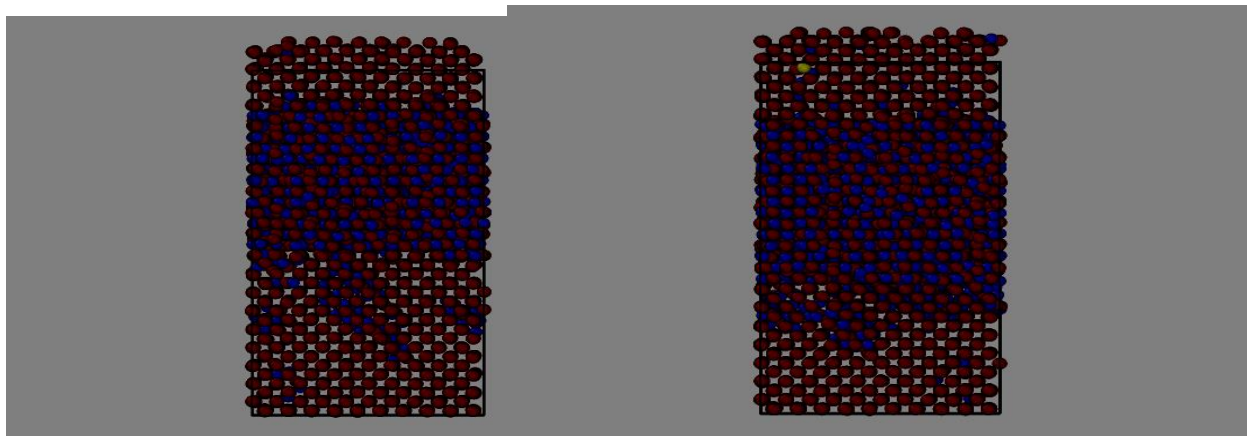
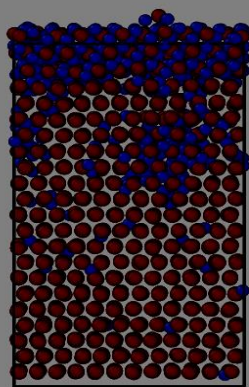
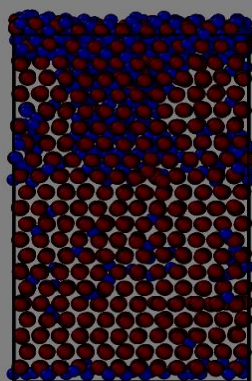


Figure 8. Surface morphology of W cells after 2000 10% Ne-90% D co-bombardments at different impact energies, for a surface temperature of 800K. The W atoms are represented by red spheres, D atoms and Ne impurities are smaller light blue and yellow spheres, respectively. (For interpretation of the references to color in this figure legend, the reader is referred to the web version of this article.)

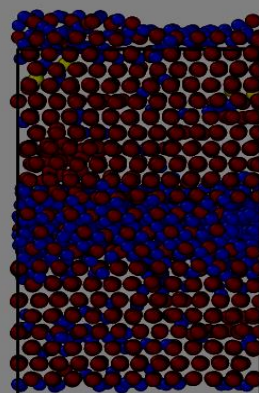
30 eV



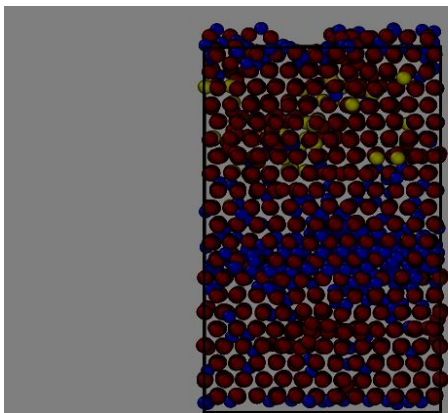
50 eV



100 eV



150 eV



200 eV

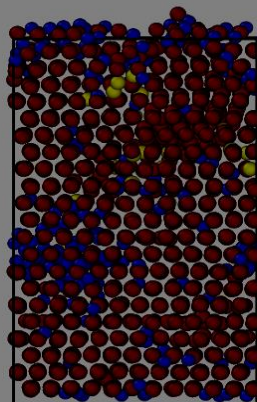


Figure  
9.  
Surface

morphology of Be cells after 2000 20% Ar-80% D co-bombardments at different impact energies, for surface temperature of 600K. The Be atoms are represented by red spheres, D atoms and Ar impurities are smaller light blue and yellow spheres, respectively. (For interpretation of the references to color in this figure legend, the reader is referred to the web version of this article.)

- [1] J. Doggett, et al. , ITER Tokamak Device, International Atomic Energy Agency, Vienna, 1991.
- [2] ITER Physics Basis Editors, ITER Physics Expert Group Chairs, Co-Chairs, ITER Joint Central Team, and Physics Integration Unit. Iter physics basis, Nuclear Fusion 39 (1999) 2137–2638
- [3] R. A. Pitts, et al. A full tungsten divertor for ITER: Physics issues and design status. J. Nucl. Mater. 438 (2013) 48-56
- [4] G. Federici 2006 Plasma wall interactions in ITER Phys. Scr. T 124 1–8
- [5] S. Brezinsek, M.F. Stamp, D. Nishijima, D. Borodin, S. Devaux, K. Krieger, S. Marsen, M. O'Mullane, C. Bjoerkas, A. Kirschner and JET EFDA contributors. NF. 54 (2014) 103001
- [6] A Kreter, et al., Erosion, formation of deposited layers and fuel retention for beryllium under the influence of plasma impurities, Physica Scripta, Volume 2014, Number T159
- [7] Parker R, Janeschitz G, Pacher H D, Post D, Chioocchio S, Federici G and Ladd P 1997 Plasma–wall interactions in ITER J. Nucl. Mater. 241–243 1–26
- [8] A. Kallenbach, M. Balden, R. Dux, T. Eich, C. Giroud, A. Huber, et al., J. Nucl. Mater. 415 (2011) S19–S26.
- [9] T. Nakano, N. Asakura, H. Kubo, J. Nucl. Mater. 438 (2013) S291–S296.
- [10] M. Ishida, H.T. Lee, Y. Ueda. The influence of neon or argon impurities on deuterium permeation in tungsten. J. Nucl. Mater. 463 (2015) 1062–1065
- [11] K. Vörtler, C. Björkas and K. Nordlund The effect of plasma impurities on the sputtering of tungsten carbide J. Phys.: Condens. Matter 23 (2011) 085002 (8pp)
- [12] R.P. Doerner, C. Björkas, D. Nishijima, T. Schwarz-Selinger, J. Nucl. Mater. 438 (2013) 272– 275.

- [13] C. Björkas, K. Nordlund, J. Nucl. Mater. 439 (2013) 174–179.
- [14] C. Björkas, D. Borodin, A. Kirschner, R.K. Janev, D. Nishijima, R. Doerner, K. Nordlund, Plasma Phys. Controlled Fusion 55 (2013) 074004.
- [15] C. Björkas, K. Vörtler, K. Nordlund, D. Nishijima, R. Doerner, New J. Phys. 11 (2009) 123017.
- [16] A. Lasa, K. Schmid, K. Nordlund, Phys. Scr. T159 (2014) 014059.
- [17] E. Safi, C. Björkas, A. Lasa, K. Nordlund, I. Sukuba, M. Probst. J. Nucl. Mat. 463 (2015) 805–809
- [18] S. Brezinsek, JET-EFDA contributors. J. Nucl. Mater. 463 (2015) 11–21
- [19] K. Nordlund, PARCAS computer code, 2006.
- [20] Juslin N, Erhart P, Träskelin P, Nord J, Henriksson K O E, Nordlund K, Salonen E and Albe K 2005 Analytical interatomic potential for modelling non-equilibrium processes in the W–C–H system J. Appl. Phys. 98 123520
- [21] C. Björkas, N. Juslin, H. Timko, K. Vörtler, K. Henriksson, K. Nordlund, P. Erhart, J. Phys.: Condens. Matter 21 (2009) 445002.
- [22] Ziegler J F, Biersack J P and Littmark U 1985 The Stopping and Range of Ions in Matter (New York: Pergamon)
- [23] H.J.C. Berendsen, J.P.M. Postma, W.F. Van Gunsteren, A. DiNola, J.R. Haak, J. Chem. Phys. 81 (8) (1984) 3684–3690.
- [24] K. Vörtler, K. Nordlund, J. Phys. Chem. C 114 (2010) 5382–5390.
- [25] P. Träskelin, K. Nordlund, J. Keinonen. J. Nucl. Mater. 357 (2006) 1–8